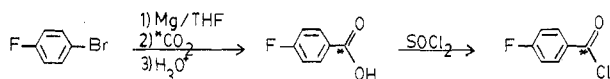


CORRESPONDENCE

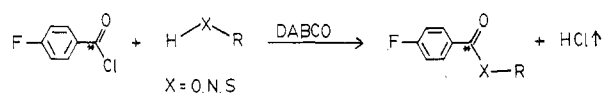
Carbon-13 and Fluorine-19 Nuclear Magnetic Resonance Chemical Shift Studies of Carbon-13 Enriched *p*-Fluorobenzoyl Derivatives

Sir: Recently Dorn and co-workers (1) have reported the use of *p*-fluorobenzoyl chloride as a ^{19}F NMR tagging reagent for characterizing molecules with active hydrogen functional groups. The base catalyzed reaction of *p*-fluorobenzoyl chloride has provided a convenient method for ^{19}F NMR analysis of alcohols, phenols, carboxylic acids, amines, and thiols. More recently, the *p*-fluorobenzoyl chloride reagent has been used to characterize biological systems such as steroids and amino acids (2). In most cases, the *p*-fluorobenzoyl derivatives provide a simple and usually quantitative method for introducing a fluorine tagging group. An attractive feature of this fluorinating reagent is the large ^{19}F chemical shift range (~ 10 ppm) for a large number of *p*-fluorobenzoate derivatives (1). Furthermore, derivatives for chemical classes (e.g., phenols, alcohols, amines, etc.) have fairly well resolved chemical shifts regions. Nevertheless, in more complex mixtures and larger substrates, spectral overlap in the ^{19}F spectrum can still be a problem.

In this paper, we shall demonstrate another spectral dimension of the *p*-fluorobenzoyl chloride tagging reagent, that is, its potential use as a dual tag (e.g., ^{19}F and ^{13}C nuclei). This is accomplished by enriching the carbonyl carbon to a level of 90% with the ^{13}C isotope. The ^{13}C enriched *p*-fluorobenzoyl chloride can be synthesized as outlined below:



There have been a number of fluorine-19 NMR tagging reagents reported in the literature during the last several years (3-8). However, ^{13}C -enriched *p*-fluorobenzoyl chloride is one of the first examples of a dual tagging reagent for analysis of molecules containing active hydrogen functional groups. The general reaction is



In this paper, we report the ^{13}C and ^{19}F chemical shifts for a limited model study of alcohols, phenols, and amine derivatives.

EXPERIMENTAL SECTION

Apparatus. The ^{13}C nuclear magnetic resonance (NMR) spectra were obtained utilizing a JEOL FX-200Q NMR spectrometer operating at 50.10 MHz. The NMR spectrometer was used with an internal deuterium lock system operating at 30.36 MHz. For all ^{13}C NMR spectra, the ^{13}C chemical shifts were internally referenced to the middle peak of chloroform-*d* and referred to tetramethylsilane by the following relationship: $\delta_{\text{C}} = 77.00 \text{ ppm} + \delta_{\text{C}_{\text{obsd}}}$ (Table I).

All ^{19}F NMR spectra were obtained utilizing a JEOL FX-60QS NMR spectrometer operating at 56.20 MHz. The NMR spectrometer used an internal deuterium lock system operating at 9.4 MHz. For the ^{19}F NMR spectra, 1,2-difluorotetrachloroethane (Peninsular Chem. Research or Aldrich Chemical Co.) was used as the ^{19}F chemical shift reference with chloroform-*d* as the solvent. Chemical shifts (δ_{F}) were measured in parts per million (ppm)

Table I. ^{13}C and ^{19}F Chemical Shift Data for *p*-Fluorobenzoate Derivatives^c

sample	$\delta_{\text{C}}1^a$	$\delta_{\text{F}}2^b$
1-butanol	165.59	-38.86
2-butanol	165.49	-38.65
2-methyl-2-propanol	164.37	-39.69
1-propanol	165.59	-38.81
phenethyl alcohol	165.43	-38.54
benzhydrol	164.44	-37.98
benzyl alcohol	165.35	-38.29
<i>p</i> -methoxybenzyl alcohol	165.44	-38.39
2-octanol	165.15	-39.11
cholesterol	164.44	-38.90
<i>n</i> -butylamine	166.37	-41.50
<i>sec</i> -butylamine	166.85	-41.59
diethylamine	170.21	-44.11
<i>n</i> -ethyl- <i>n</i> -butylamine	170.40	-44.16
carbazole	166.85	-40.38
phenol	169.19	-37.23
<i>m</i> -phenylphenol	169.48	-36.90
benzoic acid	161.26	-35.05

^aThe ^{13}C chemical shifts were internally referenced to the middle peak of chloroform-*d* and referred in the table to tetramethylsilane by the following relationship, $\delta_{\text{C}} = 77.0 \text{ ppm} + \delta_{\text{C}}(\text{observed})$. ^bThe ^{19}F chemical shifts were referenced to 1,2-difluorotetrachloroethane. ^cIncreasing positive δ_{C} and δ_{F} values denote a decrease in shielding.

with a negative value indicating shielding relative to the reference.

Preparation of ^{13}C -Enriched *p*-Fluorobenzoyl Chloride.

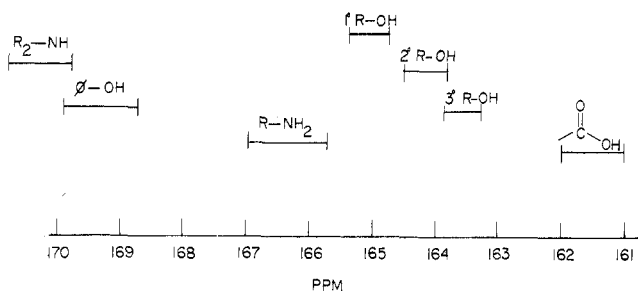
The *p*-fluorophenylmagnesium bromide was prepared by adding 0.12 mol (2.90 g) of magnesium turnings to a 250-mL flame-dried flask surmounted with a condenser and under nitrogen via a vacuum line. To this was added 25 mL of anhydrous tetrahydrofuran (THF) (distilled from lithium aluminum hydride) and two to three crystals of I_2 . A solution of 50 mL of THF and 0.12 mol (21.0 g) of *p*-fluorobromobenzene (Aldrich) was added dropwise to the magnesium turnings via an additional funnel. The Grignard reaction was started with 3-5 mL of the halide solution. After the reaction was initiated, the remaining *p*-fluorobromobenzene solution was added over a 30-min period of time with gentle heating. After addition of the halide, the mixture was stirred for 1 h under nitrogen.

Utilizing a vacuum line apparatus, 90% ^{13}C enriched $^{13}\text{CO}_2$ was generated from 0.12 mol (23.68 g) of $\text{Ba}^{13}\text{CO}_3$ by slowly adding 2.4 mol (126 mL) of concentrated H_2SO_4 . The liberated $^{13}\text{CO}_2$ was condensed immediately into the flask containing the *p*-fluorophenylmagnesium bromide, which was cooled to -196°C via a liquid nitrogen bath. The $^{13}\text{CO}_2$ was transferred to the flask containing the *p*-fluorophenylmagnesium bromide. The flask was then slowly warmed to -60°C via a xylene/liquid nitrogen bath. The $^{13}\text{CO}_2$ was rapidly absorbed by the solution at this temperature. This mixture was stirred at -60°C for 1.5 h and slowly warmed to room temperature. The mixture was stirred an additional 3 h.

After the mixture was stirred, 100 mL of 3 N HCl and ice was added to the reaction mixture which immediately formed separated aqueous-oil layers. The oil was extracted from the aqueous layer with three, 200-mL portions of ethyl ether. The solvent was concentrated in vacuo to yield a white solid. This solid was redissolved in ethyl ether and extracted with 200 mL of 1.5 N NaOH. The aqueous layer was acidified again with 3 N HCl to

Table II. ^{13}C and ^{19}F Chemical Shift Comparison Data for Various *p*-Fluorobenzyl Derivatives

sample	δ_{C}^a	diff, ppm	δ_{F}^a	diff, ppm	
<i>n</i> -butanol	165.59		-38.86		^{13}C chemical shifts overlap, but ^{19}F chemical shifts are different
isobutyl alcohol	165.49	0.1	-38.65	0.21	
<i>p</i> -methoxybenzyl alcohol	165.44		-39.39		
phenethyl alcohol	165.43	0.01	-38.54	0.15	^{19}F chemical shifts overlap, but ^{13}C chemical shifts are different
<i>n</i> -butylamine	166.37	0.48	-41.50	0.09	
<i>sec</i> -butylamine	166.85		-41.59		
diethylamine	170.21	0.19	-44.11	0.05	
<i>n</i> -ethyl- <i>n</i> -butylamine	170.40		-44.16		

^aSee Table I.Figure 1. The range of carbonyl ^{13}C chemical shifts for *p*-fluorobenzoyl derivatives.

a pH of 1. A white solid precipitated during the addition of the aqueous HCl. The solid was extracted with three, 100-mL portions of ethyl ether. The solvent was dried over anhydrous MgSO_4 and removed in vacuo to yield 14.09 g (83.9% yield) of *p*-fluorobenzoic acid. The product was used without further purification.

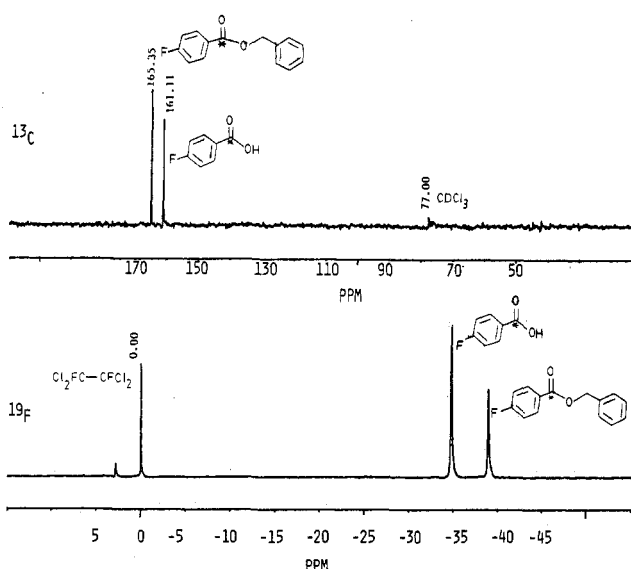
To 100 mL of tetrahydrofuran was added 0.07 mol (10 g) of ^{13}C -enriched *p*-fluorobenzoic acid and 0.091 mol (0.23 g) of I_2 . To this solution 0.28 mol (21 mL) of thionyl chloride was slowly added under nitrogen. The mixture was stirred under reflux for 15 h. The product was purified by vacuum distillation (bp 88–90 °C at 20 mmHg). A yield of 10.2 g (90%) of ^{13}C -enriched *p*-fluorobenzoyl chloride was obtained.

Derivatives of ^{13}C -enriched *p*-fluorobenzoyl chloride were prepared according to previously described procedures (1).

RESULTS AND DISCUSSION

The ^{13}C and ^{19}F chemical shifts for a number of ^{13}C -enriched derivatives of alcohols, phenols, amines, and carboxylic acids are reported in Table I. The range of ^{13}C chemical shifts for the carbonyl group of the ester, amide, and anhydride derivatives is ~ 9 ppm. Characteristic ^{13}C chemical shift regions were observed for ester, amides, and anhydride derivatives, as illustrated in Figure 1. Figure 2 illustrates the ^{19}F and ^{13}C spectra for the *p*-fluorobenzoate derivative of benzyl alcohol. In each case, the ^{19}F and ^{13}C spectra were obtained using 20 accumulations. This figure illustrates the separate spectral domains (i.e., ^{19}F and ^{13}C spectra) obtainable by this approach.

A crucial problem in complex mixture analysis is chemical shift overlap in both chemical shift domains. Table II compares the ^{19}F and ^{13}C (carbonyl) chemical shifts for several model systems obtained from Table I. As indicated, the two discrete compounds present in a complex mixture may have approximately the same ^{19}F chemical shifts (*n*-butylamine, -41.50 ppm; *sec*-butylamine, -41.59 ppm), but in this case they have significantly different ^{13}C (carbonyl) chemical shifts (166.37 and 166.85 ppm, respectively). The converse case is also illustrated; for example, *p*-methoxy benzyl alcohol and phenethyl alcohol have approximately the same ^{13}C (carbonyl) chemical shifts but are distinguished by separate ^{19}F chemical shifts.

Figure 2. The decoupled ^{19}F and ^{13}C spectra for the *p*-fluorobenzoate derivative of benzyl alcohol.

In summary, from this limited model study, a chemical shift range of ~ 9 ppm is observed for both ^{19}F and ^{13}C derivatives. The remarkable feature of these data is the fact that ^{19}F chemical shifts are not attenuated relative to the ^{13}C chemical shifts even though the ^{19}F nuclide is five more bonds removed from these structural changes. These data reflect the known facile ability for transmission of substituent effects to the para position (9) in substituted aromatic systems.

Registry No. *p*-Fluorobenzoyl chloride (^{13}C enriched), 91742-47-1; 1-butanol, 71-36-3; 2-butanol, 78-92-2; 2-methyl-2-propanol, 75-65-0; 1-propanol, 71-23-8; phenethyl alcohol, 60-12-8; benzhydrol, 91-01-0; benzyl alcohol, 100-51-6; *p*-methoxybenzyl alcohol, 105-13-5; 2-octanol, 123-96-6; cholesterol, 57-88-5; *n*-butylamine, 109-73-9; *sec*-butylamine, 13952-84-6; diethylamine, 109-89-7; *n*-ethyl-*n*-butylamine, 13360-63-9; carbazole, 86-74-8; phenol, 108-95-2; *m*-phenylphenol, 580-51-8; benzoic acid, 65-85-0; 1-butanol *p*-fluorobenzoate deriv., 91742-48-2; 2-butanol *p*-fluorobenzoate deriv., 91742-49-3; 2-methyl-2-propanol *p*-fluorobenzoate deriv., 91742-50-6; 1-propanol *p*-fluorobenzoate deriv., 91742-51-7; phenethyl alcohol *p*-fluorobenzoate deriv., 91742-52-8; benzhydrol *p*-fluorobenzoate deriv., 91742-53-9; benzyl alcohol *p*-fluorobenzoate deriv., 91742-54-0; *p*-methoxybenzyl alcohol *p*-fluorobenzoate deriv., 91742-55-1; 2-octanol *p*-fluorobenzoate deriv., 91742-56-2; cholesterol *p*-fluorobenzoate deriv., 91742-57-3; *n*-butylamine *p*-fluorobenzoate deriv., 91742-58-4; *sec*-butylamine *p*-fluorobenzoate deriv., 91742-59-5; diethylamine *p*-fluorobenzoate deriv., 91742-60-8; *n*-ethyl-*n*-butylamine *p*-fluorobenzoate deriv., 91742-61-9; carbazole *p*-fluorobenzoate deriv., 91742-62-0; phenol *p*-fluorobenzoate deriv., 91742-63-1; *m*-phenylphenol *p*-fluorobenzoate deriv., 91742-64-2; benzoic acid *p*-fluorobenzoate deriv., 91742-65-3.

LITERATURE CITED

- (1) Spratt, M. P.; Dorn, H. C. *Anal. Chem.* **1984**, *56*, 2038-2043.
- (2) Spratt, M. P.; Meng, Y.; Dorn, H. C. *Anal. Chem.* **1985**, *57*, 76-81.
- (3) Slevi, P.; Glass, T. E.; Dorn, H. C. *Anal. Chem.* **1979**, *57*, 1931-1934.
- (4) Manatt, S. L. *J. Am. Chem. Soc.* **1966**, *88*, 1323-1324.
- (5) Leader, G. R. *Anal. Chem.* **1973**, *45*, 1700-1706.
- (6) Koller, K. L.; Dorn, H. C. *Anal. Chem.* **1982**, *54*, 529-533.
- (7) Zuber, G. E.; Staiger, D. B.; Warren, R. J. *Anal. Chem.* **1983**, *55*, 64-67.
- (8) Shue, F. F.; Yen, T. F. *Anal. Chem.* **1982**, *54*, 1641-1642.
- (9) Taft, R. W.; Prosser, F.; Goodman, L.; Davis, G. T. *J. Chem. Phys.* **1963**, *38*, 380-387.

¹Permanent address: Department of Chemistry, San Francisco State University, San Francisco, CA 94132.

M. P. Spratt
D. Armistead
E. Motell¹
H. C. Dorn*

Department of Chemistry
Virginia Polytechnic Institute and State University
Blacksburg, Virginia 24061

RECEIVED for review April 13, 1984. Accepted July 3, 1984.

On the Identification of the Sulfur Oxidation State in Inorganic Sodium Sulfoxy Salts by Laser Microprobe Mass Analysis and Secondary Ion Mass Spectrometry

Sir: In a recent paper (1), Bruynseels and Van Grieken investigated the potential of laser microprobe mass spectrometry (LAMMA) to infer the sulfur-to-oxygen stoichiometry in various sodium sulfoxy salts. Previously we carefully studied (2-5) such inorganic compounds in static and dynamic secondary ion mass spectrometry (SIMS); Ganjei et al. also reported negative spectra in the dynamic mode (6). It is thus interesting to compare SIMS and LAMMA regarding the metalloid's oxidation state identification and to examine the various ion formation mechanisms which likely occur in both techniques.

LAMMA and SIMS exhibit qualitatively the same positive ions, especially with respect to the pseudomolecular region (Na_3SO_3^+ , Na_3SO_4^+). We have collected and compared in Table I the R values ($R = I_{\text{Na}_3\text{SO}_3^+}/I_{\text{Na}_3\text{SO}_4^+}$) obtained in LAMMA (1) and SIMS (5). The SIMS data include the values relative to an argon ion dose of 10^{13} ions·cm⁻² ($R_{S,13}$) and those characteristic of ion doses higher than 3×10^{15} ions·cm⁻² ($R_{S,15}$). The latter are found after the equilibrium between preferential sputtering (reduction) and recoil implantation (oxidation) of oxygen atoms is reached. The redox phenomena which influence deeply the SIMS spectra of most inorganic oxygenated salts were analyzed and discussed in ref 5 while in ref 4 the formation mechanisms of the Na_3SO_n^+ ($n = 3, 4$) secondary ions were investigated by using labeled ¹⁸O.

To determine the ability to infer the sulfur oxidation state, one can define a factor of merit F which is the ratio of $R_{\text{Na}_2\text{SO}_3}$ to $R_{\text{Na}_2\text{SO}_4}$. From Table I, F is calculated to be about 3 either in LAMMA or in SIMS at low ion doses. Although the factor of merit is the same, it is nevertheless striking that in SIMS the "parent" molecular peak is the most intense among the two characteristic cluster ions and this, whichever is the primary ion dose. On the contrary, in LAMMA, Na_3SO_4^+ is the most intense in both sulfite and sulfate.

Regarding the influence of the energy deposited by the primary beam (photons or ions) on the ratio R , LAMMA and SIMS behave differently. According to the work reported in ref 1, the R_L values are rather little sensitive to the laser energy; they could decrease slightly as the power increases if any actual effect exists. It seems likely that, in LAMMA, the larger the laser energy, the easier it is to identify the sulfur oxidation state. On the contrary, in SIMS, we showed (see, for instance, Figures 4 and 5 in ref 5) that an increase in the deposited energy makes the determination of the valence state more risky. As a matter of fact, the unambiguous discrimination between S^{4+} and S^{6+} is performed easily only at low

Table I. Values of the Intensity Ratio R ($R = I_{\text{Na}_3\text{SO}_3^+}/I_{\text{Na}_3\text{SO}_4^+}$)

salt	$R_{L,0.7}^a$	$R_{L,3.9}^a$	$R_{S,13}^b$	$R_{S,15}^c$
Na_2SO_3	0.84 ± 0.03	0.74 ± 0.06	1.85 ± 0.05	1.14 ± 0.05
Na_2SO_4	0.28 ± 0.04	0.10 ± 0.04	0.65 ± 0.05	0.70 ± 0.05

^a R_L = values obtained in LAMMA (ref 1) for a laser energy of either 0.7 μJ or 3.9 μJ ; R_S = values obtained in SIMS (ref 5) after an ion dose of 10^{13} ions·cm⁻² or 3×10^{15} ions·cm⁻².

doses ($< 10^{13}$ ions·cm⁻²) and low argon ion energy (< 0.8 keV). For instance, argon ions of 3 keV energy would lead to a wrong identification of Na_2SO_4 at low doses (up to 6×10^{13} ions·cm⁻²). A reliable measurement can be made when the steady state is reached but with a worse factor of merit (1.6 instead of 3).

The similarities and discrepancies pointed out above are most valuable for shedding some light on the cluster ion formation mechanisms in both techniques. Two mechanisms can explain the cluster ion emission in LAMMA and SIMS of polyatomic solids: direct ejection and recombination. In the direct ejection model, a lattice fragment is ejected intact (nearest neighborhood is kept); afterward it can only suffer possible unimolecular dissociation before detection. The recombination model means that, after atomization up to various degrees, particles (neutrals, ions, atoms, aggregates) recombine in the gas phase. The factors which govern each of the processes are different. It is likely that the intact ejection of a lattice fragment occurs if the energy involved is low enough to avoid complete atomization. This supports the idea that, in SIMS, intact molecular ions could originate from cascade tails. In such a model, some of the weakest bonds in the crystal have to be broken preferentially. Consequently, in such a case, the main parameter, which governs the ion pattern, is the relative strength of the bonds between the lattice atoms. Regarding sodium sulfoxy salts, the weakest interaction is likely between sodium and oxygen (the relative strengths of the interactions between lattice atoms are estimated according to bond dissociation energies found in ref 7), this can lead to a relatively high yield of intact anions (SO_n^-). Contrary to LAMMA (1), SIMS (6) enables the identification of the sulfur oxidation state if the Plog model (8) is used to fit the SO_n^- distribution. The fact that it does not work in LAMMA is perhaps related to a higher degree of atomization owing to a higher deposited energy density. The negative ion patterns of the oxygenated sulfur (or nitrogen) salts should be very